

THE
GEORGE
WASHINGTON
UNIVERSITY

ATIONS OF CRACK GROWTH AND PLASTICITY
FINITE ELEMENT ANALYSIS

STUDENTS FACULTY STUDY R
ESEARCH DEVELOPMENT FUT
URE CAREER CREATIVITY CC
MMUNITY LEADERSHIP TECH
NOLOGY FRONTIER DESIGN
ENGINEERING APP ENC
GEORGE WASHINGTON UNIV

19960229 000

DTIC QUALITY INSPECTED 1

SCHOOL OF ENGINEERING
AND APPLIED SCIENCE



PLASTEC

CONSIDERATIONS OF CRACK GROWTH AND PLASTICITY IN
FINITE ELEMENT ANALYSIS

James D. Lee and Harold Liebowitz

July, 1978

School of Engineering and Applied Science
The George Washington University
Washington, D.C. 20052

ABSTRACT

A finite element analysis was made of crack growth in a center-cracked specimen subjected to monotonically increasing load until the point of fast fracture. Since part of the specimen experienced unloading, the boundary value problem which was formulated was based upon incremental theory of plasticity. Experimental load and crack-size records were utilized. Linear relations between plastic energy and crack growth were observed. Fracture toughness parameters \tilde{G}_c , which were evaluated at the onset of unstable crack propagation, obtained from finite element analysis were in good agreement with those determined experimentally.


1. Introduction

Linear elastic fracture mechanics is widely used by research workers and engineers as a tool to determine fracture toughness, K_c or \bar{G}_c , for evaluating the susceptibility of engineering materials to unstable fracture. Since ductile materials have higher resistance to crack growth than brittle materials, the recent trend is to develop more ductile materials for structural applications. However, ductile materials show a considerable amount of crack-tip plasticity and significant amount of crack growth prior to the onset of unstable fracture.

A plastic zone correction [1,2], the J-integral [3,4] and COD methods [5] have been proposed to treat fracture involving crack-tip plasticity in the absence of crack growth. Further, the crack growth resistance curve method [6] has been proposed for cases having subcritical crack growth. Liebowitz and Eftis [7,8] introduced the nonlinear energy method which is applicable to semibrittle fracture. Jones et al [9] developed a corresponding experimental program to determine the toughness parameter \tilde{G}_c and Liebowitz et al [10] provided theoretical and experimental comparisons between their nonlinear energy method and other existing methods. Recently Jones et al [11] used four empirical methods to determine \tilde{G}_c in the range of crack growth.

In this work, a finite element analysis is developed for crack growth problems based upon incremental theory of plasticity.

In this paper, mention is made of the work of Newman [12] whose crack growth criterion is based on crack-tip strain with element-mesh size being a parameter, and that of de Koning [13] who found crack tip opening angle as constant during the process of crack growth. In this analysis, the realistic experimental curve relating load and crack size is taken as an input. In order to demonstrate the validity of this work, the numerical output of load and displacement is compared to its experimental counterpart. Moreover, a linear relation is observed between plastic energy and crack size during the process of crack growth. The finite-element values of \tilde{G}_c , based upon empirical methods derived by Jones et al [11], are in good agreement with the experimental values.



2. Stress-Strain Relations

In linear elasticity, the stress-strain relations for a homogeneous isotropic material can be written in either of the following forms [14]:

$$\sigma_{ij} = \lambda \epsilon_{kk} \delta_{ij} + 2\mu \epsilon_{ij} , \quad (2.1)$$

$$\epsilon_{ij} = \frac{1}{2\mu} \sigma_{ij} - \frac{\lambda}{2\mu(3\lambda + 2\mu)} \sigma_{kk} \delta_{ij} , \quad (2.2)$$

where λ and μ are the Lamé constants, σ_{ij} and ϵ_{ij} are the stress tensor and strain tensor respectively. Introducing stress deviator s_{ij} as follows:

$$s_{ij} \equiv \sigma_{ij} - \frac{1}{3} \sigma_{kk} \delta_{ij} , \quad (2.3)$$

(2.2) can be rewritten as:

$$E\epsilon_{ij} = (1 + \nu) s_{ij} + \frac{1 - 2\nu}{3} \sigma_{kk} \delta_{ij} , \quad (2.4)$$

where E and ν are Young's modulus and Poisson's ratio respectively.

In nonlinear elasticity, adopting the model suggested by Ramberg and Osgood, we generalize the stress-strain relations as follows:

$$E\epsilon_{ij} = (1 + \nu) s_{ij} + \frac{1 - 2\nu}{3} \sigma_{kk} \delta_{ij} + \frac{3}{2} \alpha \sigma_e^{n-1} s_{ij} , \quad (2.5)$$

where the effective stress σ_e is defined as:

$$\sigma_e^2 \equiv \frac{3}{2} s_{ij} s_{ij} . \quad (2.6)$$

In simple tension test, namely, all stress components are zero except $\sigma_{11} = \sigma$, we obtain the following nonvanishing components of ϵ_{ij} , s_{ij} and the effective stress:

$$\begin{aligned} E\epsilon_{11} &= \sigma + \alpha \sigma^n, \\ E\epsilon_{22} &= E\epsilon_{33} = -\nu\sigma - \frac{1}{2} \alpha \sigma^n, \\ s_{11} &= \frac{2}{3} \sigma, \\ s_{22} &= s_{33} = -\frac{1}{3} \sigma, \\ \sigma_e &= \sigma. \end{aligned} \quad (2.7)$$

For the theory of incremental plasticity, a certain portion of the material is said to be in an unloading situation if its current effective stress σ_e is less than the maximum effective stress σ_e^* it experienced before, otherwise it is said to be in a loading situation. The relations between incremental stresses and incremental strains in the loading situation can be derived from eqn. (2.5) as follows:

$$\begin{aligned} E d\epsilon_{ij} &= (1+\nu) ds_{ij} + \frac{1-2\nu}{3} d\sigma_{kk} \delta_{ij} \\ &+ \frac{3}{2} \alpha \sigma_e^{n-1} ds_{ij} + \frac{9}{4} \alpha(n-1) \sigma_e^{n-3} s_{ij} s_{kl} ds_{kl}. \end{aligned} \quad (2.8)$$

In the unloading situation, we assume the incremental stress-strain relations are the same as those in linear elasticity, i.e.,

$$E d\epsilon_{ij} = (1+\nu) ds_{ij} + \frac{1-2\nu}{3} d\sigma_{kk} \delta_{ij}. \quad (2.9)$$

The stress-strain relation in the case of simple tension is illustrated graphically in Fig. 1. In the case of generalized

plane stress, eqn. (2.8) may be written in the following matrix form:

$$\begin{bmatrix} d\epsilon_x \\ d\epsilon_y \\ d\gamma_{xy} \end{bmatrix} = \begin{bmatrix} h_{11} & h_{12} & h_{13} \\ h_{12} & h_{22} & h_{23} \\ h_{13} & h_{23} & h_{33} \end{bmatrix} \begin{bmatrix} d\sigma_x \\ d\sigma_y \\ d\sigma_{xy} \end{bmatrix}, \quad (2.10)$$

where

$$\begin{aligned} h_{11} &= \{1 + g + h(2\sigma_x - \sigma_y)^2\}/E, \\ h_{12} &= \{-v - g/2 + h(2\sigma_x - \sigma_y)(2\sigma_y - \sigma_x)\}/E, \\ h_{13} &= 6h(2\sigma_x - \sigma_y)\sigma_{xy}/E, \\ h_{22} &= \{1 + g + h(2\sigma_y - \sigma_x)^2\}/E, \\ h_{23} &= 6h(2\sigma_y - \sigma_x)\sigma_{xy}/E, \\ h_{33} &= \{2(1+v) + 3g + 36h\sigma_{xy}^2\}/E, \end{aligned}$$

and

$$g \equiv \alpha\sigma_e^{n-1}, \quad h \equiv \alpha(n-1)\sigma_e^{n-3}/4.$$

Equivalently, eqn. (2.10) can be expressed as

$$\begin{bmatrix} d\sigma_x \\ d\sigma_y \\ d\sigma_{xy} \end{bmatrix} = \begin{bmatrix} d_{11} & d_{12} & d_{13} \\ d_{12} & d_{22} & d_{23} \\ d_{13} & d_{23} & d_{33} \end{bmatrix} \begin{bmatrix} d\epsilon_x \\ d\epsilon_y \\ d\gamma_{xy} \end{bmatrix}, \quad (2.11)$$

where matrix $[d_{ij}]$ is the inverse of matrix $[h_{ij}]$. In the case of unloading, we have

$$\begin{pmatrix} d\sigma_x \\ d\sigma_y \\ d\sigma_{xy} \end{pmatrix} = \frac{E}{1-\nu^2} \begin{pmatrix} 1 & \nu & 0 \\ \nu & 1 & 0 \\ 0 & 0 & (1-\nu)/2 \end{pmatrix} \begin{pmatrix} d\epsilon_x \\ d\epsilon_y \\ d\gamma_{xy} \end{pmatrix}. \quad (2.12)$$

3. Strain Energy

In the case of a simple tension test, if the specimen is first loaded monotonically from $\sigma = 0$ to $\sigma = \sigma^*$ and then unloaded monotonically from $\sigma = \sigma^*$ to $\sigma = 0$, we obtain the following strain components:

$$\begin{aligned}\epsilon_{11} \equiv \epsilon &= \int_0^{\sigma^*} d\epsilon_{11} + \int_{\sigma^*}^0 d\epsilon_{11} \\ &= \int_0^{\sigma^*} \frac{1}{E} [1 + \alpha \sigma^{n-1}] d\sigma + \int_{\sigma^*}^0 \frac{1}{E} d\sigma \\ &= \frac{1}{E} \{ [1 + \alpha \sigma^{n-1}] \sigma^* - \sigma^* \} \\ &= \frac{1}{E} \alpha \sigma^{*n},\end{aligned}\tag{3.1}$$

$$\begin{aligned}\epsilon_{22} = \epsilon_{33} \equiv \hat{\epsilon} &= \int_0^{\sigma^*} d\epsilon_{22} + \int_{\sigma^*}^0 d\epsilon_{22} \\ &= \int_0^{\sigma^*} \frac{1}{E} [-\nu - \frac{1}{2} \alpha \sigma^{n-1}] d\sigma + \int_{\sigma^*}^0 \frac{-\nu}{E} d\sigma \\ &= -\frac{1}{2} \alpha \sigma^{*n} / E.\end{aligned}\tag{3.2}$$

Note that, in evaluating the first and second integral of eqns. (3.1-3.2), the general incremental stress-strain relations (2.8) and (2.9) are utilized respectively. $\epsilon_{11} = \epsilon$ and $\epsilon_{22} = \epsilon_{33} \equiv \hat{\epsilon}$

so obtained in eqns. (3.1-3.2) are called plastic strains which are the residuals after the applied load is removed. Comparing eqns. (3.1-3.2) with eqn. (2.7)₁ and eqn. (2.7)₂, we may rewrite eqn. (2.5) as

$$E\epsilon_{ij} = E(\epsilon_{ij}^e + \epsilon_{ij}^p) , \quad (3.3)$$

where the elastic strains ϵ_{ij}^e and plastic strains ϵ_{ij}^p are

$$E\epsilon_{ij}^e = (1+\nu)s_{ij} + \frac{1-2\nu}{3}\sigma_{kk}\delta_{ij} ,$$

$$E\epsilon_{ij}^p = \frac{3}{2}\alpha\sigma_e^{n-1}s_{ij} .$$

Now suppose, in a general case, the loading and unloading history of a certain portion of the material can be divided into two stages. In the first stage the effective stress σ_e increases monotonically to σ_e^* which corresponds to σ_{ij}^* and in the second stage the effect stress decreases monotonically to $\hat{\sigma}_e$ which corresponds to $\hat{\sigma}_{ij}$. Then the strain energy density ϕ can be obtained as:

$$\begin{aligned} \phi &\equiv \int_0^{\sigma_e^*} \sigma_{ij} d\epsilon_{ij} + \int_{\sigma_e^*}^{\hat{\sigma}_e} \sigma_{ij} d\epsilon_{ij} \\ &= \frac{1}{E} \left\{ \frac{1+\nu}{3} \hat{\sigma}_e^2 + \frac{1-2\nu}{6} (\hat{\sigma}_{kk})^2 + \frac{n}{n+1} \alpha \sigma_e^{*n+1} \right\} . \end{aligned} \quad (3.4)$$

we notice the strain energy density can be separated into two parts:

$$\phi_e = \frac{1}{E} \left\{ \frac{1+\nu}{3} \hat{\sigma}_e^2 + \frac{1-2\nu}{6} (\hat{\sigma}_{kk})^2 \right\} , \quad (3.5)$$

$$\phi_p = \frac{n}{E(n+1)} \alpha \sigma_e^{*n+1} , \quad (3.6)$$

where the elastic strain energy density ϕ_e is a function of the current stresses $\hat{\sigma}_{ij}$ and the plastic strain energy density ϕ_p is a function of maximum effective stress σ_e^* . The irreversible and dissipative nature of plastic strain energy density is indicated in eqn. (3.6). In two dimensional problems, the elastic- and plastic-strain energy per unit thickness over an area A can be obtained as:

$$U_e \equiv \int_A \phi_e \, dA, \quad (3.7)$$

$$U_p \equiv \int_A \phi_p \, dA. \quad (3.8)$$

4. Center-Cracked Specimen

In this work, we focus our attention on a rectangular plate of length 2ℓ , width $2w$, and thickness B , with a centered line crack of initial crack size $2a_0$ subjected to symmetric boundary conditions (cf. Fig. 2). Therefore only the first quadrant of the plate $R = [x, y | 0 \leq x \leq w, 0 \leq y \leq \ell]$ needs to be analyzed. Experimentally one may obtain a curve of applied stress σ vs crack size. A realistic experimental curve relating σ and a is shown in Fig. 3. We are interested in the investigation of the process that crack size slowly increases from $a = a_0$ to $a = a_c$ as the applied stress increases from $\sigma = 0$ to $\sigma = \sigma_c$. Suppose we have two adjacent states: $\sigma = \sigma^{(1)}$ and $a = a^{(1)}$ at State 1, $\sigma = \sigma^{(2)}$ and $a = a^{(2)}$ at State 2. Correspondingly, the boundary conditions may be specified as (cf. Fig. 4):

$$\sigma_x = k\sigma^{(i)}, \quad \sigma_{xy} = 0 \text{ on } S_1 \equiv [x = w, 0 \leq y \leq \ell], \quad (4.1)$$

$$\sigma_y = \sigma^{(i)}, \quad \sigma_{xy} = 0 \text{ on } S_2 \equiv [y = \ell, 0 \leq x \leq w], \quad (4.2)$$

$$u_x = 0, \quad \sigma_{xy} = 0 \text{ on } S_3 \equiv [x = 0, 0 \leq y \leq \ell], \quad (4.3)$$

$$\sigma_y = 0, \quad \sigma_{xy} = 0 \text{ on } S_4 \equiv [y = 0, 0 \leq x \leq a^{(i)}], \quad (4.4)$$

$$u_y = 0, \quad \sigma_{xy} = 0 \text{ on } S_5 \equiv [y = 0, a^{(i)} \leq x \leq w]. \quad (4.5)$$

In other words, the boundary conditions associated with the process from State 1 to State 2 can be expressed as (cf. Fig. 5):

$$\delta\sigma_x = k[\sigma^{(2)} - \sigma^{(1)}], \quad \delta\sigma_{xy} = 0 \text{ on } S_1, \quad (4.6)$$

$$\delta\sigma_y = \sigma^{(2)} - \sigma^{(1)}, \quad \delta\sigma_{xy} = 0 \text{ on } S_2, \quad (4.7)$$

$$\delta u_x = 0, \quad \delta\sigma_{xy} = 0 \text{ on } S_3, \quad (4.8)$$

$$\delta\sigma_y = 0, \quad \delta\sigma_{xy} = 0 \text{ on } \Gamma_1 \equiv [y = 0, 0 \leq x \leq a^{(1)}], \quad (4.9)$$

$$\delta\sigma_y = -\bar{\sigma}_y, \quad \delta\sigma_{xy} = 0 \text{ on } \Gamma_2 \equiv [y = 0, a^{(1)} \leq x \leq a^{(2)}], \quad (4.10)$$

$$\delta u_y = 0, \quad \delta\sigma_{xy} = 0 \text{ on } \Gamma_3 \equiv [y = 0, a^{(2)} \leq x \leq w], \quad (4.11)$$

where $\bar{\sigma}_y$ is the stress of State 1 distributed along $y = 0$ between $a^{(1)} \leq x \leq a^{(2)}$.

If we have the solutions of State 1, then, for any given adjacent state specified by $\sigma^{(2)}$ and $a^{(2)}$, the boundary conditions for the transition from State 1 to State 2 are well defined in eqns. (4.6-4.11). The equations of equilibrium and the strain-displacement relations in the incremental form can be written as:

$$\delta\sigma_{ij,i} = 0, \quad (4.12)$$

$$\delta\epsilon_{ij} = \frac{1}{2}(\delta u_{i,j} + \delta u_{j,i}). \quad (4.13)$$

Eqns. (4.6-4.13) with eqn. (2.8) and/or eqn. (2.9) mathematically define the crack growth problem as a boundary value problem. After the boundary value problem is solved, the stresses, strains, and displacements at State 2 may be obtained as

$$\sigma_{ij}^{(2)} = \sigma_{ij}^{(1)} + \delta\sigma_{ij} , \quad (4.14)$$

$$\epsilon_{ij}^{(2)} = \epsilon_{ij}^{(1)} + \delta\epsilon_{ij} , \quad (4.15)$$

$$u_i^{(2)} = u_i^{(1)} + \delta u_i . \quad (4.16)$$

Following the same procedure, one may analyze stepwise the whole process of slow crack growth up to the onset of fast crack propagation.

5. Finite Element Procedure

Let a finite element mesh with N_p nodal points and N_e triangular elements be set up in region $R = [x, y | 0 \leq w, 0 \leq y \leq \ell]$. In this work, $N_p = 300$, $N_e = 518$, and a series of very fine elements are being distributed along the path of slow crack growth. The area of those elements is in the order of $10^{-6}w\ell$. If j is the number of a certain nodal point, then u_{2j-1} and u_{2j} are the displacement of that point in x and y direction respectively, f_{2j-1} and f_{2j} are the corresponding external concentrated force components acting on that point. The displacement field within each triangular element is assumed to be linear with respect to the coordinates. Therefore the strain field, and accordingly the stress field, within each triangular element are constant. For each element (cf. Fig. 6), let the incremental strain field $[\delta\epsilon]$, incremental stress field $[\delta\sigma]$, and incremental nodal point displacements $[\delta]$ be represented by

$$[\delta\epsilon] \equiv [\delta\epsilon_x, \delta\epsilon_y, \delta\gamma_{xy}]^T, \quad (5.1)$$

$$[\delta\sigma] \equiv [\delta\sigma_x, \delta\sigma_y, \delta\sigma_{xy}]^T, \quad (5.2)$$

$$[\delta] \equiv [\delta u_{2i-1}, \delta u_{2i}, \delta u_{2j-1}, \delta u_{2j}, \delta u_{2k-1}, \delta u_{2k}]^T. \quad (5.3)$$

Then we have

$$[\delta\epsilon] = [B][\delta], \quad (5.4)$$

$$[\delta\sigma] = [d][\delta\epsilon],$$

where $[d]$ is a 3×3 matrix as indicated in eqns. (2.11) and (2.12) which are valid for loading and unloading respectively, and

$$[B] = \frac{1}{2\Delta} \begin{vmatrix} b_i & 0 & b_j & 0 & b_k & 0 \\ 0 & c_i & 0 & c_j & 0 & c_k \\ c_i & b_i & c_j & b_j & c_k & b_k \end{vmatrix}, \quad (5.5)$$

$$2\Delta \equiv \det \begin{vmatrix} 1 & x_i & y_i \\ 1 & x_j & y_j \\ 1 & x_k & y_k \end{vmatrix}, \quad (5.6)$$

$$b_i \equiv y_j - y_k, \quad c_i \equiv -x_j + x_k, \quad (5.7)$$

with the other coefficients obtained by a cyclic permutation of subscripts in the order of i, j, k . The stiffness matrix per unit thickness of this triangular element linking incremental forces and incremental displacements may be obtained as [15,16]:

$$[k] = [B]^T [d] [B] A, \quad (5.8)$$

where A is the area of the element. Finally the governing equation can be written as:

$$\sum_{\beta=1}^{2N_p} K_{\alpha\beta} \delta u_{\beta} = \delta f_{\alpha}, \quad \alpha = 1, 2, \dots, 2N_p \quad (5.9)$$

where the $2N_p \times 2N_p$ stiffness matrix $[K]$ is equal to the sum of N_e local stiffness matrices $[k]_I$, $I = 1, \dots, N_e$.

As matrix $[d]$ of each element depends on the current stresses when that element is in a loading situation, the matrix $[K]$ also depends on the whole stress field. Thus, an iteration process has to be taken to solve the nonlinear matrix equation (5.9). The iteration process could be described as follows. Suppose, in a step by step process, we have the solutions of State 1, (i.e., for each element we have the current stresses σ_{ij} and the maximum effective stress σ_e^*). Then, for each element, we guess at the stresses $\hat{\sigma}_{ij}$ of State 2. Then the current effective stress σ_e and the effective stress $\hat{\sigma}_e$ may be obtained respectively from

$$\sigma_e = (\sigma_x^2 + \sigma_y^2 - \sigma_x \sigma_y + 3\sigma_{xy}^2)^{\frac{1}{2}}, \quad (5.10)$$

$$\hat{\sigma}_e = (\hat{\sigma}_x^2 + \hat{\sigma}_y^2 - \hat{\sigma}_x \hat{\sigma}_y + 3\hat{\sigma}_{xy}^2)^{\frac{1}{2}}. \quad (5.11)$$

The corresponding matrix $[d]$ for each element may be found from one of the three following cases:

$$(1) \quad \sigma_e = \sigma_e^* \text{ and } \hat{\sigma}_e > \sigma_e^*$$

For case (1), the element is in a loading situation; matrix $[d]$ is assumed to be the average matrix corresponding to two states of stresses, i.e.,

$$d_{ij} = \frac{1}{2}[d_{ij}(\sigma) + d_{ij}(\hat{\sigma})]. \quad (5.12)$$

$$(2) \quad \sigma_e \leq \sigma_e^* \text{ and } \hat{\sigma}_e \leq \sigma_e^*$$

For case (2), the element is in an unloading situation; matrix [d] should be the same as indicated in eqn. (2.12).

$$(3) \quad \sigma_e < \sigma_e^* \text{ and } \hat{\sigma}_e > \sigma_e^*$$

For case (3), the element has experienced unloading and is being loaded again, the matrix [d] is obtained as

$$d_{ij} = f d_{ij}(\hat{\sigma}) + (1-f) d_{ij}(0), \quad (5.13)$$

where

$$f \equiv (\hat{\sigma}_e - \sigma_e^*) / (\hat{\sigma}_e - \sigma_e), \quad (5.14)$$

and $d_{ij}(0)$ denotes the matrix corresponding to vanishing stress state.

After solving eqn. (5.9), one may obtain the calculated stresses $\bar{\sigma}_{ij}$ and its corresponding effective stress $\bar{\sigma}_e$. The iteration process will be continued until, for each element, the guessed stresses and calculated stresses are approximately the same and the averaged percentage difference between $\hat{\sigma}_e$ and $\bar{\sigma}_e$ is below certain allowable values of error. After the iteration process is completed, it is straightforward to calculate quantities of interest in fracture mechanics.

6. Dissipated Energy and Crack Growth

The irreversible and dissipative nature of plastic strain energy density have been indicated in Sec. 3. After the iteration process for a certain incremental step is completed, we have the correctly guessed stresses $\hat{\sigma}_{ij}$ and the corresponding effective stress $\hat{\sigma}_e$ of a new state for each finite element. If the newly obtained effective stress is larger than the maximum effective stress σ_e^* obtained in the previous states, one should replace σ_e^* by $\hat{\sigma}_e$, which will be used as the maximum effective stress for the next incremental step. Now we recall the expressions for elastic and plastic strain energy density as follows:

$$\phi_e = \frac{1}{E} \left\{ \frac{1+\nu}{3} \hat{\sigma}_e^2 + \frac{1-2\nu}{6} (\hat{\sigma}_{kk})^2 \right\}, \quad (6.1)$$

$$\phi_p = \frac{n}{E(n+1)} \alpha \sigma_e^{*n+1}. \quad (6.2)$$

We notice that ϕ_e depends on the current stresses and therefore demonstrates its elastic nature. On the other hand, ϕ_p is a monotonically increasing quantity because σ_e^* is always increasing, this corresponds to the irreversibility of plasticity and the dissipative nature of plastic energy. After the finite element analysis for each incremental step is completed, it is straightforward to obtain the total plastic energy P (per unit thickness) for the whole region R as follows:

$$P = \sum_{i=1}^{N_e} (\phi_p A)_i \quad . \quad (6.3)$$

For a stationary crack problem, the crack size is regarded as a given quantity and hence the question is to determine the critical load at the onset of slow crack growth. However, as the crack starts to grow in a stable situation, one has to treat crack size as a variable. Strictly speaking, one more variable corresponds to one more governing equation for the system. Before one can establish a governing equation for crack size, the relation between crack size and other fracture parameter has to be proposed and tested [12,13]. Motivated by the Griffith's concept [17,18] that surface energy is proportional to its area, and the energy for the new fracture surface has to be supplied from the released strain energy of the specimen, we decided to take the energy approach. Since crack growth is generally regarded as a irreversible process and crack size is an ever increasing quantity, we propose that crack growth is a function of plastic energy, i.e.,

$$a - a_0 = f(P) \quad . \quad (6.4)$$

We mention that Broberg [19] proposed a similar concept which can be expressed as:

$$dU_0/da = dD_0/da \quad , \quad (6.5)$$

where U_0 is the energy flow to the process region and D_0 is the energy dissipation in the process region. However Broberg's

engineering approach is based on the so called approximate path-independence of J-integral even in the cases of crack growth.

After we analyze a realistic crack growth problem with all the input data obtained experimentally, we observe the following fact:

$$a - a_0 = \beta(P - P_0) \quad (6.5)$$

which means the amount of crack growth is linearly proportional to the increment of plastic energy. The normalized plastic energy per unit thickness $p \equiv PE/\sigma_Y^2 w^2$ is plotted against normalized crack size $c \equiv a/w$ in Fig. 7. The correlation coefficient attains a high value of 0.9997. Eqn. (6.5) may be rewritten as

$$\begin{aligned} P &= P_0 + (a - a_0)/\beta \\ &= (P_0 - a_0/\beta) + \frac{1}{\beta} a \end{aligned} \quad (6.6)$$

7. Fracture Toughness

Liebowitz and Eftis [7,8] developed a nonlinear energy method to evaluate the toughness parameter \tilde{G}_C from a single load-displacement record for cases of no crack growth. The method may be briefly described as follows. First, let the experiment load-displacement record be represented by

$$v = \frac{F}{M} + k \left(\frac{F}{M} \right)^n, \quad (7.1)$$

where v is the load point displacement, F is the load, $1/M$ is the crack size dependent elastic compliance, n and k are constants. Then for a given critical load F_C , one may obtain a dimensionless quantity \tilde{C} representing the nonlinearity as follows:

$$\tilde{C} = 1 + \frac{2nk}{n+1} \left(\frac{F_C}{M} \right)^{n-1} \quad (7.2)$$

The nonlinear toughness parameter \tilde{G}_C is obtained as:

$$\tilde{G}_C = \tilde{C} \bar{G}_C, \quad (7.3)$$

where \bar{G}_C is the corresponding linear elastic fracture toughness and may be obtained by using Irwin's G-K relation, i.e.,

$$\bar{G}_C = K_C^2 / E. \quad (7.4)$$

And K_C is determined using the following polynomial expression for center-cracked specimen [20]

$$K_C = \sigma_C \sqrt{\pi a} \left[1 - 0.1 \frac{a}{w} + \left(\frac{a}{w} \right)^2 \right]. \quad (7.5)$$

Jones et al [11] further developed four different methods to account for the effect of subcritical crack growth. We briefly

describe these four methods and in each method we compare the experimental value of \tilde{G}_C with the numerical value of \tilde{G}_C obtained by finite-element analysis.

Method 1

The experimental part of this method can be separated into two steps: (1) to determine \tilde{C} from the experimental load displacement record, (2) to calculate \tilde{G}_C by eqns. (7.4-7.5) using actual critical stress σ_C and initial crack size. For illustrative purpose, we take specimen #11 (2024-T3) as an example and the data for that specimen are listed below:

$$\begin{aligned} 2w &= 12 \text{ in. ,} \\ 2a_0 &= 6 \text{ in. ,} \\ 2\ell &= 32 \text{ in. ,} \\ E &= 10300 \text{ ksi,} \\ \nu &= 0.33 , \\ \sigma_Y &= 55.04 \text{ ksi ,} \\ n &= 6.025 , \\ \alpha \sigma_Y^{n-1} &= 2.207 . \end{aligned} \tag{7.6}$$

And load-crack size relation is plotted in Fig. 3, which is taken as an input in this work. As an output the numerical data for load-displacement curve obtained by finite element analysis are plotted in Fig. 8 to compare with the experimental curve. In this particular case we have

$$\tilde{G}_c \text{ (Exp)} = 521 \text{ lb/in.}, \quad \tilde{G}_c \text{ (FE)} = 473 \text{ lb/in.} \quad (7.7)$$

The difference is about 10%; 2% comes from the calculation of \bar{G}_c due to fact that eqn.(7.5) always gives higher value for K_c , and hence higher value for \bar{G}_c from eqn. (7.4) and 8% comes from the calculation of \tilde{C} due to the discrepancy between finite-element and experimental data in the load-displacement record.

Method 2

The experimental part of this method involves the determination of a hypothetical load-displacement curve assuming there is no crack growth. Eftis et al. [12] propose that

$$\bar{F} = F_c M(a_0)/M(a_c) \quad (7.8)$$

being used as the critical load corresponding to the hypothetical load-displacement curve. Lee and Liebowitz [22] developed a computer program which can be used to analyze a center-cracked specimen in the nonlinear range without crack growth, and therefore it is straightforward to find \bar{F} assuming critical displacement v_c to be the same as obtained experimentally. We find that

$$\begin{aligned} \tilde{G}_c \text{ (FE)} &= \tilde{C} \text{ (FE)} \bar{G}_c \text{ (FE)} \\ &= 1.1325 \times 381.77 (14.01/12.8)^2 \\ &= 518 \text{ lb/in.} \end{aligned} \quad (7.9)$$

No experimental value for \tilde{G}_c has been reported by Jones et al [11].

Method 3

The experimental part of this method involves the determination of M_0 , n_0 , k_0 , and \tilde{C} accordingly, from the portion of load-displacement curve, which has no crack growth, and the value of \bar{F} from the following equation

$$v_c = \frac{\bar{F}}{M_0} + k_0 \left(\frac{\bar{F}}{M_0} \right)^{n_0} \quad (7.10)$$

The experimental value of \tilde{G}_c is reported to be 520 lb/in. and the finite-element value of \tilde{G}_c is found to be 519.7 lb/in.

Method 4

Utilizing k_0 and n_0 obtained in Method 3, we recall eqn. (7.1) and write as follows

$$v_c = \frac{F_c}{M_c} + k_0 \left(\frac{F_c}{M_c} \right)^{n_0}, \quad (7.11)$$

which is used to determine $M_c \equiv M(a_c)$. The experimental part of this method is to determine \tilde{C} . based upon M_c , n_0 , k_0 , F_c , and \bar{G}_c , based upon critical crack size a_c . The experimental value of \tilde{G}_c is reported to be 581 lb/in. However, we found that \tilde{G}_c (FE) = 491.6 lb/in., which we believe is more reliable. In summary, the finite-element values of \tilde{G}_c for four different methods are 473, 518, 519.7 491.6 comparing with experimental values 521, - , 520, 581 respectively.

8. Conclusions

In this work, we focused our attention on the finite element analysis of crack growth in a center-cracked specimen subjected to monotonically increasing loads until fast fracture occurs. During the process of crack extension, although the applied load is increased monotonically, part of the specimen has experienced unloading. Therefore, in this work the boundary value problem formulated is based upon incremental theory of plasticity.

Since, in a crack growth problem, crack size is no longer a given constant parameter and must be treated as a variable, a governing equation for crack size is needed. Before we can formulate such a governing equation, an experimental curve relating load and crack size is taken as an input and hopefully from the output one may find the relation between crack size and other fracture parameters derivable from the stress field. Because of the irreversible and dissipative nature of plasticity and crack growth, we believe that crack size should be related to plastic energy. Indeed, after the completion of the analysis, we do observe the fact that the amount of crack growth is linearly proportional to the increment of plastic energy. In another study of ours which is in progress, the linear relation, will be employed as an input replacing the experimental load-crack size curve. If the result yields a load-crack size curve which is in agreement with the corresponding experi-

mental, are then one may claim a governing equation for crack size.

Another aspect which is of concern is the fracture toughness parameter \tilde{G}_c . Liebowitz and his coworkers [8-10] developed a nonlinear energy method and its corresponding experimental procedure for the determination of \tilde{G}_c at the onset of stable crack growth. Recently Jones et al [11] presented four different empirical methods to account for the effect of subcritical crack growth. These methods enable us to determine the fracture toughness parameter \tilde{G}_c at the onset of unstable crack propagation based upon the experimental load-displacement record. Then the finite-element values which were determined for \tilde{G}_c were compared to the corresponding experimental values; satisfactory agreement was found.

The following points should be stressed. Inputs for the computer program include the material constants α and n , in addition to Young's modulus E and Poisson's ratio ν , determined from the simple tension test of unnotched specimen. However, as a matter of fact, α and n vary over a wide range when one tries to describe the experimental stress-strain curve by a three parameter expression and, from our experience, the finite element computer program is quite sensitive to the input α and n . We believe this is the major reason for the existing discrepancy between the experimental load-displacement curve and its finite-element counterpart, which has a 5.2% difference in displacement at the critical

load. Although there is a discrepancy, we find that the finite-element values of \tilde{G}_c based on the empirical methods have less scatter than the experimental counterparts. Generally speaking, this work provides support to the nonlinear energy method developed by Liebowitz and Eftis [7], Eftis and Liebowitz [8] and its corresponding experimental procedures Jones et al [9], Liebowitz et al [10] and Jones et al [11], in determining the fracture toughness values in the range of stable crack growth.

ACKNOWLEDGMENT

The authors wish to acknowledge financial support for this work from the Office of Naval Research (N00014-75-C-0946) and NASA-Langley Research Center (NGL 09-010-053).

REFERENCES

1. G. R. Irwin, J. A. Kies, and H. L. Smith, Proc. American Society for Testing Materials, 58, 640 (1958).
2. G. R. Irwin, NRL Report 5486 (1960).
3. J. R. Rice, Fracture V.2, ed. by Liebowitz, Academic Press, New York (1968).
4. C. P. Cherepanov, J. Appl. Math. Mech. (PMM) V. 31, No. 3 (1967).
5. A. A. Wells, Proc. Conf. Crack Propagation, Cranfield, U.K. (1962).
6. Fracture Toughness Evaluation by R-Curve Methods, ASTM STP 527, American Society for Testing Materials, Philadelphia (1973).
7. H. Liebowitz and J. Eftis, Engrg. Fract. Mech., 3, 267 (1971).
8. J. Eftis and H. Liebowitz, Engrg. Fract. Mech., 7, 101 (1975).
9. D. L. Jones, H. Liebowitz, and J. Eftis, Engrg. Fract. Mech., 6, 639 (1974).
10. H. Liebowitz, D. L. Jones, and P. K. Poulouse, Proc. of the 1974 Symposium on Mechanical Behavior of Materials, V. 1, P. 1, Society of Materials Science, Japan (1974).
11. D. L. Jones, P. K. Poulouse, J. Eftis, and H. Liebowitz, \tilde{G}_c and R-Curve Fracture Toughness Values for Aluminum Alloys Under Plane Stress Conditions, forthcoming in Engrg. Fract. Mech.

12. J. C. Newman, Jr., ASTM STP 637, American Society for testing Materials, Philadelphia (1976).
13. A. U. deKoning, Report NLR MP 75035U, National Aerospace Lab. (NLR), The Netherlands (1975).
14. I. S. Sokolnikoff, Mathematical Theory of Elasticity, McGraw-Hill, New York (1956).
15. O. S. Zienkiewicz, The Finite Element Method in Engineering Science, McGraw-Hill, London (1971).
16. L. J. Segerlind, Applied Finite Element Analysis, John Wiley & Sons, Inc., New York (1976).
17. A. A. Griffith, Phil. Trans. Roy. Soc. London, Ser. A 221, 163 (1921).
18. A. A. Griffith, Proc. of the 1st Int. Congress on Applied Mechanics, Delft, (1924).
19. K. B. Broberg, On the Treatment of the Fracture Problem at Large Scale of Yielding, presented at Int. Conf. on Fract. Mech. and Technology, Hong Kong (1977).
20. W. F. Brown, Jr. and J. E. Srawley, ASTM STP 410, American Society for Testing Materials, Philadelphia (1966).
21. J. Eftis, D. L. Jones and H. Liebowitz, Engrg. Fract. Mech., 7, 491 (1975).
22. J. D. Lee and H. Liebowitz, Engrg. Fract. Mech., 9, 765 (1977).

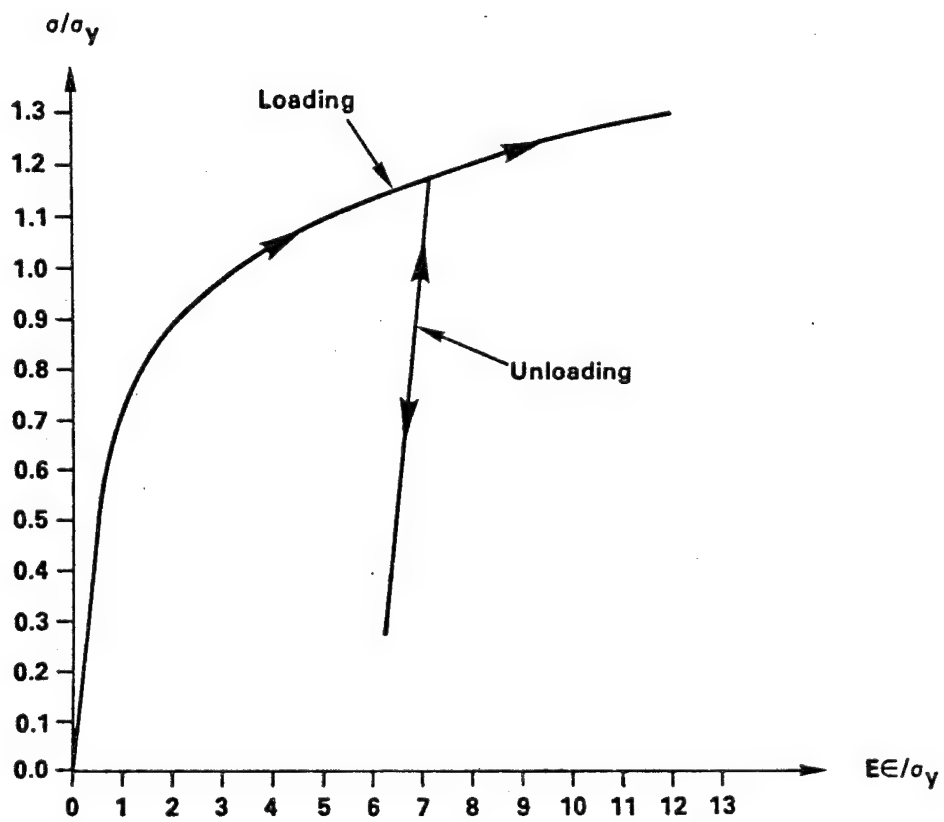


Fig.1 Stress - Strain Relation in Simple Tension Test

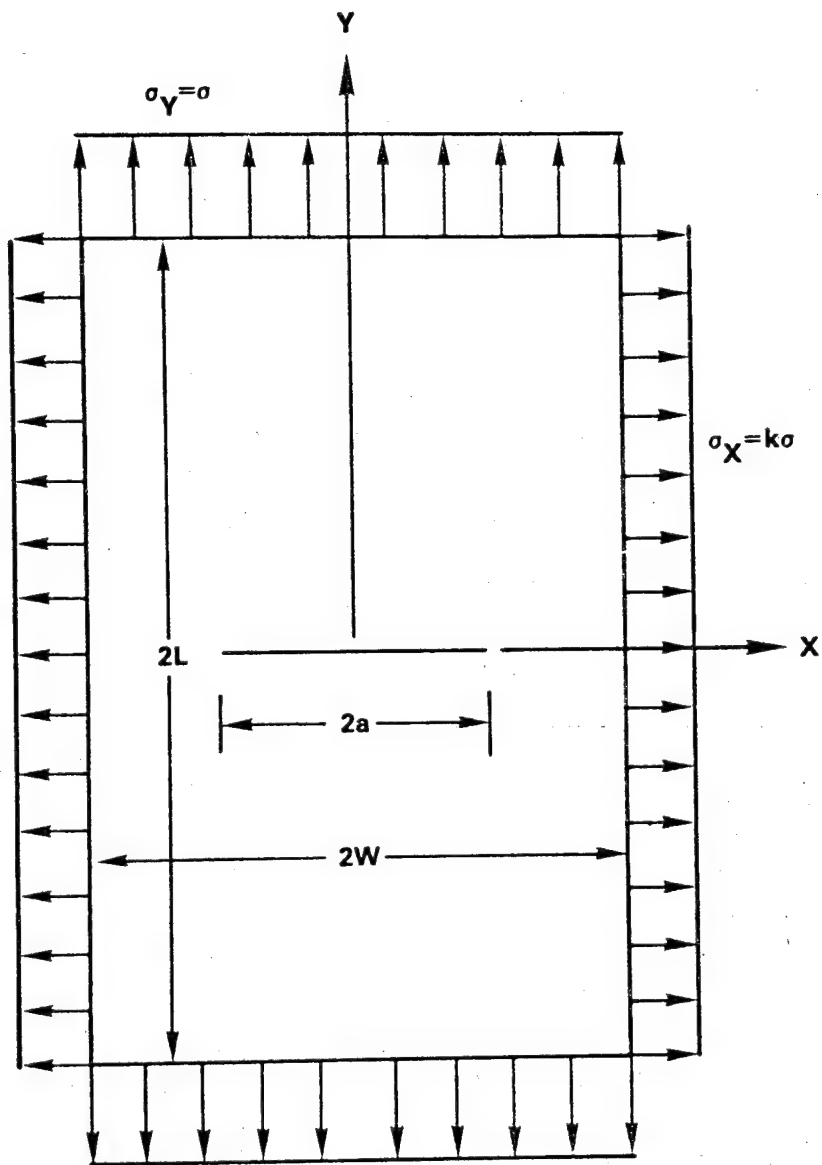


Fig. 2 Center - Cracked Specimen

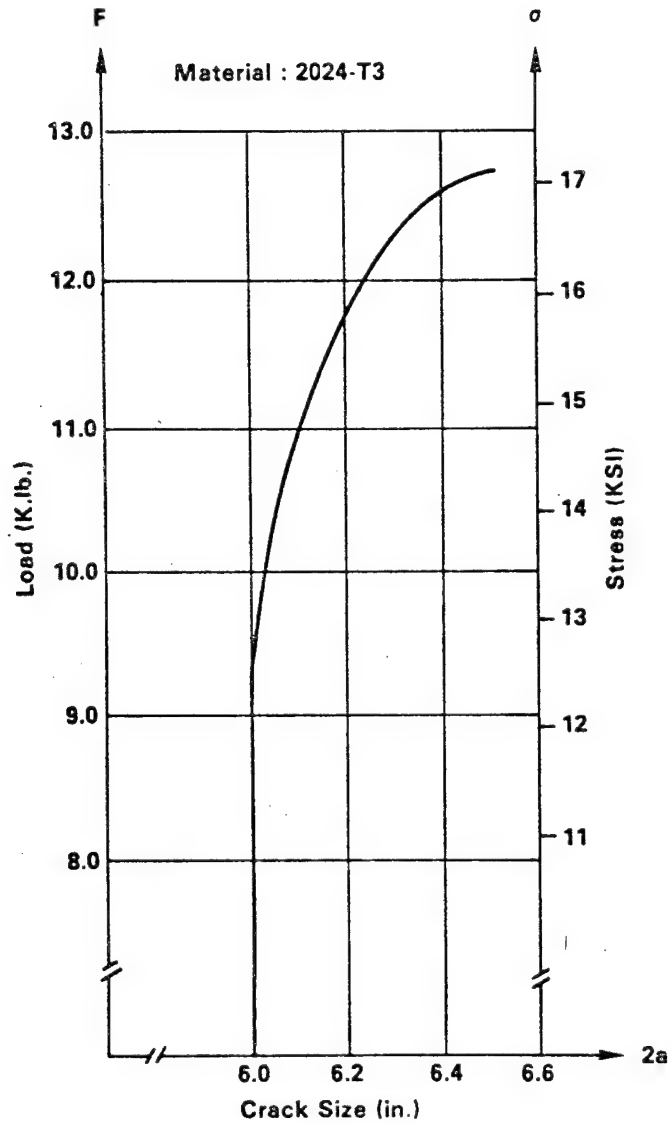


Fig. 3 Load (Stress) vs Crack Size; $2W=12$ in., $2L=32$ in.,
 $B=0.062$ in., $E=10300$ ksi, $\sigma_Y=55.04$ ksi, $n=6.025$,
 $\nu=0.33$, $\alpha \sigma_Y^{n-1}=2.207$; $k=0$

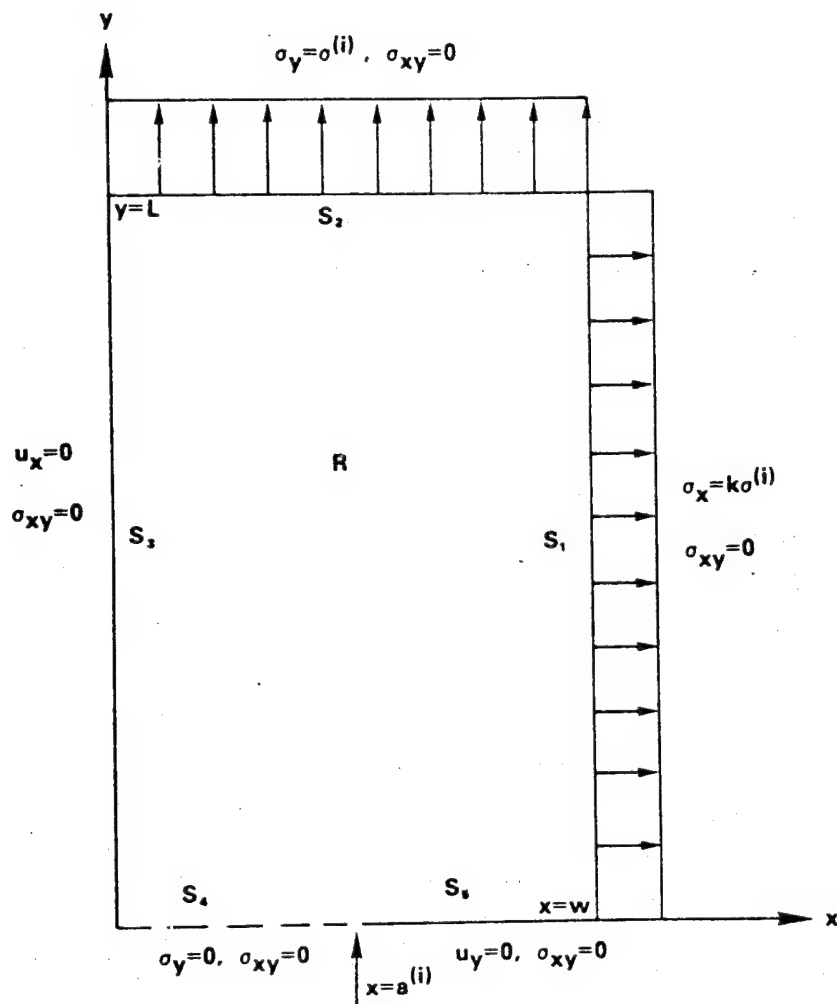


Fig. 4 Boundary Conditions of i -th State

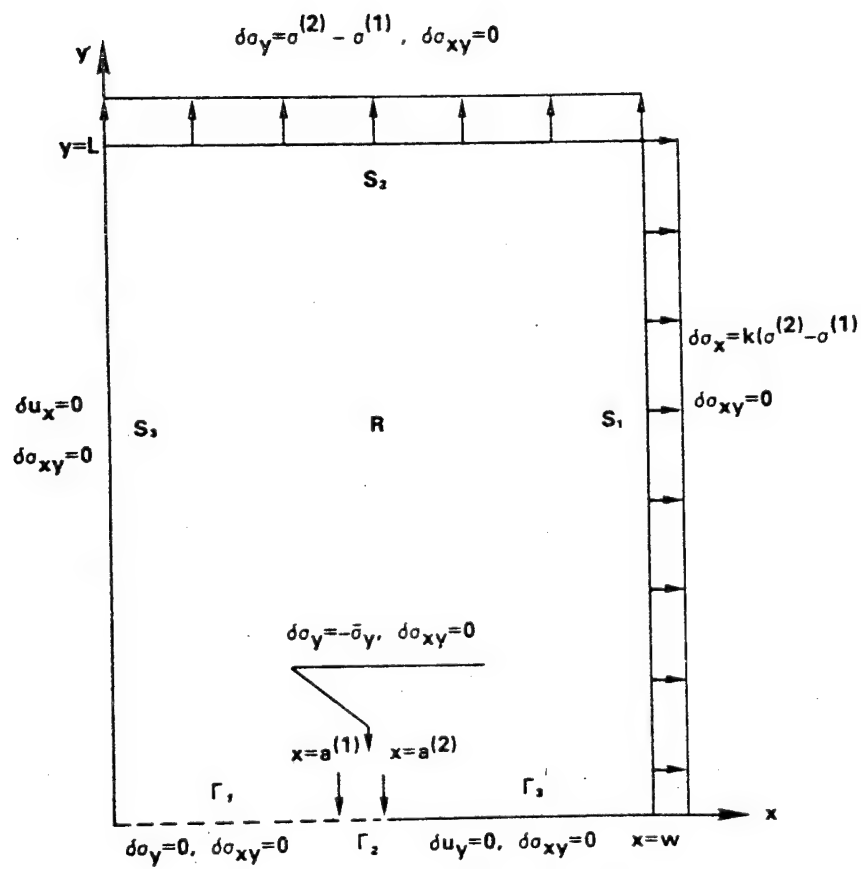


Fig. 5 Boundary Conditions of Process from State 1 to State 2

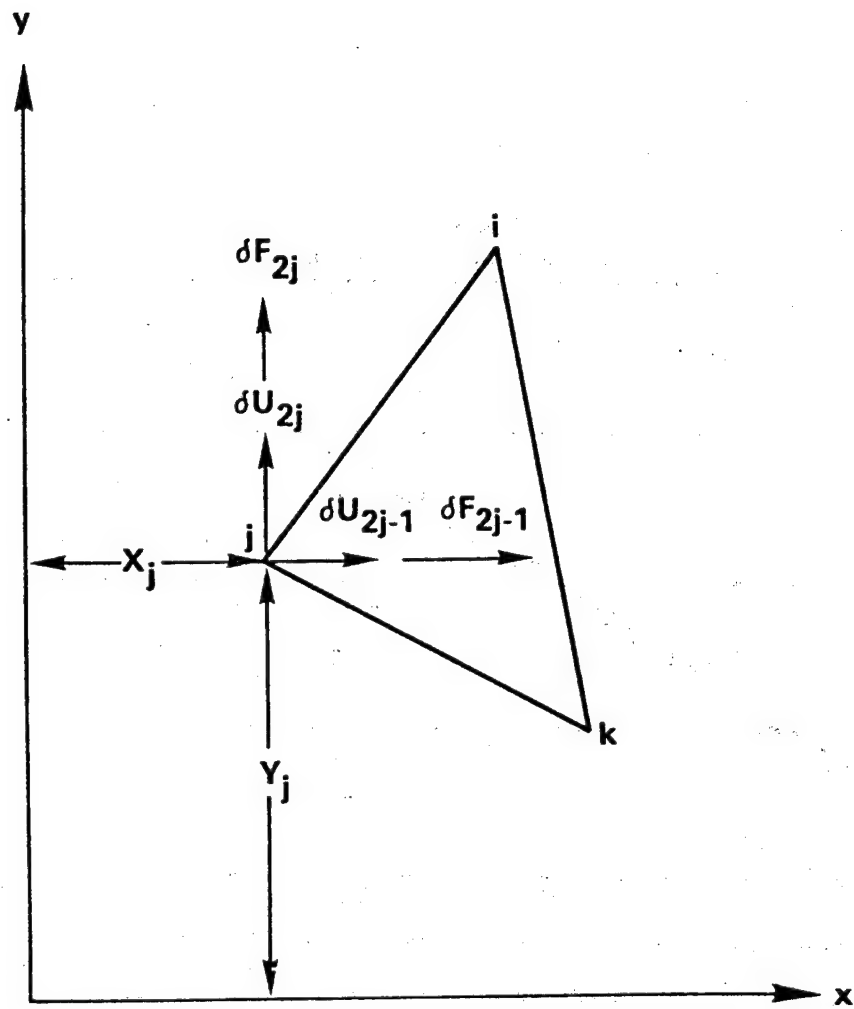


Fig. 6 Coordinates, Incremental Displacements and Forces of the j -th Nodal Point

$PE/(\sigma_y W)^2$

Material : 2024-T3

Correlation Coefficient = 0.9997

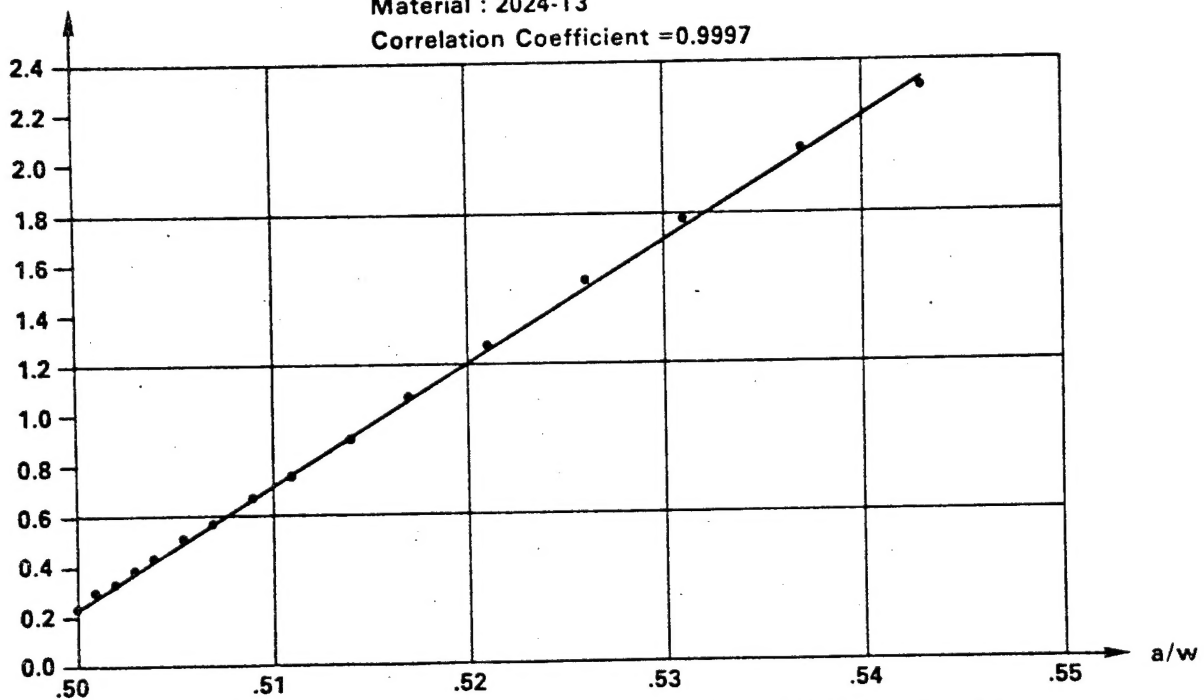


Fig. 7 Plastic Strain Energy vs Crack Size; $2w=12$ in., $2L=32$ in., $2a_0=6$ in.,

$B=0.062$ in., $E=10300$ ksi, $\nu=0.33$, $n=6.025$, $\sigma_y=55.04$ ksi, $\alpha\sigma_y^{n-1}=2.207$; $k=0$

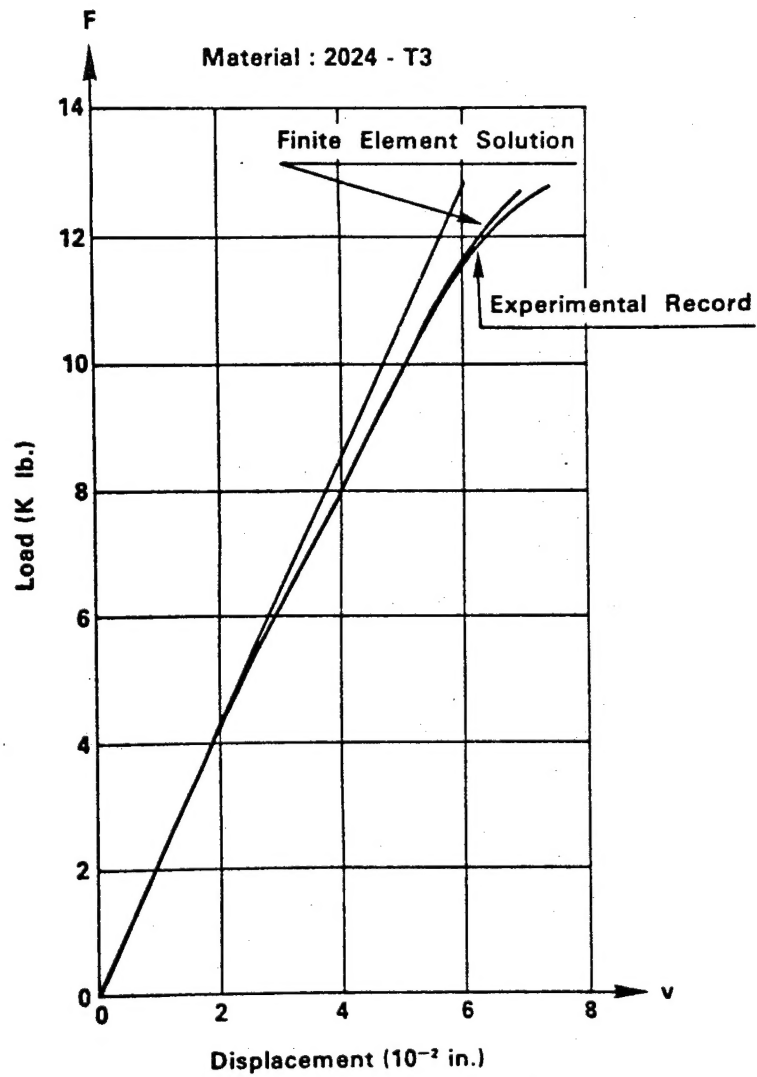


Fig. 8 Load-Displacement Curve, $2w=12$ in.,
 $2L=32$ in., $2a_0=6$ in., $B=0.062$ in.,
 $E=10300$ ksi, $\sigma_Y=55.04$ ksi, $\nu=0.33$,
 $n=6.025$, $\alpha\sigma_Y^{n-1}=2.207$; $k=0$

REPORT DOCUMENTATION PAGE		READ INSTRUCTIONS BEFORE COMPLETING FORM
1. REPORT NUMBER	2. GOVT ACCESSION NO.	3. RECIPIENT'S CATALOG NUMBER
4. TITLE (and Subtitle) Consideration of Crack Growth and Plasticity in Finite Element Analysis		5. TYPE OF REPORT & PERIOD COVERED
7. AUTHOR(s) James D. Lee and Harold Liebowitz		6. PERFORMING ORG. REPORT NUMBER
9. PERFORMING ORGANIZATION NAME AND ADDRESS School of Engineering & Applied Science The George Washington University Washington, D.C. 20052		8. CONTRACT OR GRANT NUMBER(s) NAVY 00014-75-C-0946
11. CONTROLLING OFFICE NAME AND ADDRESS Office of Naval Research Arlington, Virginia 22217		10. PROGRAM ELEMENT, PROJECT, TASK AREA & WORK UNIT NUMBERS
14. MONITORING AGENCY NAME & ADDRESS (if different from Controlling Office)		12. REPORT DATE July, 1978
		13. NUMBER OF PAGES 34
		15. SECURITY CLASS. (of this report) UNCLASSIFIED
		15a. DECLASSIFICATION/DOWNGRADING SCHEDULE
16. DISTRIBUTION STATEMENT (of this Report) Approved for Public Release: Distribution Unlimited		
17. DISTRIBUTION STATEMENT (of the abstract entered in Block 20, if different from Report)		
18. SUPPLEMENTARY NOTES		
19. KEY WORDS (Continue on reverse side if necessary and identify by block number) Fracture Mechanics Finite Element Methods Crack Growth Plasticity		
20. ABSTRACT (Continue on reverse side if necessary and identify by block number) A finite element analysis was made of crack growth in a center-cracked specimen subjected to monotonically increasing load until the point of fast fracture. Since part of the specimen experienced unloading, the boundary value problem which was formulated was based upon incremental theory of plasticity. Experimental load and crack-size records were utilized. Linear relations between plastic energy and crack growth were observed. Fracture toughness parameters G_c , which were evaluated at the onset of unstable crack propagation, obtained from finite element analysis were in good agreement with those determined experimentally.		

